Fabrication of cation-doped BaTaO2N photoanodes for efficient photoelectrochemical water splitting under visible light irradiation

AUTHOR(S):

Higashi, Masanobu; Yamanaka, Yuta; Tomita, Osamu; Abe, Ryu

CITATION:

Higashi, Masanobu ...[et al]. Fabrication of cation-doped BaTaO2N photoanodes for efficient photoelectrochemical water splitting under visible light irradiation. APL Materials 2015, 3(10): 104418.

ISSUE DATE:

2015-09-18

URL:

http://hdl.handle.net/2433/202616

Fabrication of cation-doped BaTaO2N photoanodes for efficient photoelectrochemical water splitting under visible light irradiation

Masanobu Higashi, Yuta Yamanaka, Osamu Tomita, and Ryu Abe

Citation: APL Mater. **3**, 104418 (2015); doi: 10.1063/1.4931487
View online: http://dx.doi.org/10.1063/1.4931487
View Table of Contents: http://scitation.aip.org/content/aip/journal/aplmater/3/10?ver=pdfcov
Published by the AIP Publishing

APL MATERIALS **3**, 104418 (2015)

Fabrication of cation-doped $BaTaO_2N$ photoanodes for efficient photoelectrochemical water splitting under visible light irradiation

Masanobu Higashi,[1] Yuta Yamanaka,[1] Osamu Tomita,[1] and Ryu Abe[1,2,a]
[1]*Graduate School of Engineering, Kyoto University, Katsura, Nishikyo-ku, Kyoto 615-8510, Japan*
[2]*JST-CREST, 7 Gobancho, Chiyoda-ku, Tokyo 102-0076, Japan*

(Received 22 July 2015; accepted 10 September 2015; published online 18 September 2015)

A series of cation-doped $BaTaO_2N$ particle was synthesized to control the donor density in the bulk for improving the performance of photoelectrochemical water splitting on porous $BaTaO_2N$ photoanodes under visible light. Among the dopants (Mo^{6+}, W^{6+}, Zr^{4+}, and Ti^{4+}) examined, Mo^{6+} cations can be introduced into the Ta^{5+} site up to 5 mol. % without producing any impurity phases; the donor density of $BaTaO_2N$ was indeed increased significantly by introducing higher ratio of Mo^{6+} dopant. The porous photoanodes of Mo-doped $BaTaO_2N$ showed much higher photocurrent than others including undoped one and also exhibited much improved performance in photoelectrochemical water splitting into H_2 and O_2 after loaded with cobalt oxide cocatalyst and coupled with Pt counter electrode. [http://dx.doi.org/10.1063/1.4931487]

Photoelectrochemical (PEC) water splitting using semiconductor photoelectrodes has attracted considerable attention due to the potential for the clean production of H_2 from water by utilizing solar energy, as well as photocatalytic water splitting using semiconductor particles.[1–5] The development of stable PEC water splitting systems that can harvest wide range of visible light, which represents almost half of the available solar spectrum on the earth's surface, is indispensable for achieving practically high efficiency in conversion of solar energy to H_2. A series of n-type metal (oxy)nitride semiconductors, such as TaON,[6–9] Ta_3N_5,[8,10,11] $BaTaO_2N$,[12–14] and $SrNbO_2N$,[15–17] is one of the promising materials for fabricating efficient photoanodes in such PEC systems because they possess appropriate conduction and valence band edges for both H_2 and O_2 productions as well as narrow bandgaps allowing visible light absorption; among them $BaTaO_2N$ and $SrNbO_2N$ can harvest much wider range of visible light up to ca. 660 and 680 nm, respectively. We have recently demonstrated efficient PEC water splitting under visible light using porous TaON or $BaTaO_2N$ photoanodes loaded with appropriate cocatalyst such as cobalt oxide.[18,19] In the case of $BaTaO_2N$ photoanode, preliminary treatment of $BaTaO_2N$ particles in a H_2 stream at high temperature (1073 K) was found to increase the photocurrent significantly, certainly due to the increased conductivity within the $BaTaO_2N$ bulk via the formation of anion defects such as O^{2-} or N^{3-} vacancies. However, such high temperature H_2 treatment cannot be applied for the materials that incorporate easily reduced cations such as Nb^{5+} [16] and also is undoubtedly unfavorable for the precise control of carrier density in semiconductor particles to obtain the maximal performance in PEC. Doping of guest elements has been extensively used as an effective way of controlling the carrier density in semiconductors. The enhanced PEC efficiencies via cation-doping have been indeed reported in some semiconductor photoanodes[20–26] and photocathodes,[27,28] while such reports are basically limited to metal oxide semiconductors.[20–27] For example, the partial substitution of V^{5+} cations by W^{6+} or Mo^{6+} in $BiVO_4$ semiconductor has been reported to improve the PEC performance of porous

[a]Author to whom correspondence should be addressed. Electronic mail: ryu-abe@scl.kyoto-u.ac.jp

$BiVO_4$ photoanode significantly, certainly due to the reduced electroresistance within the electrode, i.e., the increased donor density in $BiVO_4$ bulk. However, there is no report on the improved PEC performance in metal oxynitride semiconductor photoelectrodes based on carrier density control by means of cation doping, as far as the present authors know.

In the present study, we attempted to synthesis cation-doped $BaTaO_2N$ particles in which a part of penta-valent Ta^{5+} was replaced by tetra or hexahydric-valent cations (Ti^{4+}, Zr^{4+}, Mo^{6+}, and W^{6+}) to control the donor density and applied them for fabricating porous photoanodes to achieve improved PEC performance under visible light.

Cation-doped $BaTaO_2N$ particles, in which a part (x mol. %) of Ta^{5+} was decreased from the stoichiometric amount to introduce the same molar amount of tetra or hexahydric-valent cations (Ti^{4+}, Zr^{4+}, Mo^{6+}, or W^{6+}) into the Ta^{5+} sites, were prepared via thermal ammonolysis of the corresponding oxide precursors.[14,29] The metal sources were added into a methanol (30 ml) with the ratio of Ba: Ta: M = 1: $(1 - x)$: x, in which the molar amount of Ba was fixed to be 12 mmol and the x values were ranged from 2 to 7. Along with the above metal sources, 0.48 mol of ethylene glycol and 182 mmol of anhydrous citric acid were added to the methanol solution. The as-prepared solution was heated at ca. 400 K for ca. 2 h to achieve complete dissolution and also to promote esterification. The resulting resin was charred in a mantle heater for 1 h at ca. 623 K to afford a black solid mass, which was finally calcined on an Al_2O_3 plate at 773 K for 1 h in air. The as-prepared amorphous oxide precursor was then heated at 1223 K for 20 h under NH_3 flow (100 ml min^{-1}). The obtained samples will be denoted as BTON:M-x (M = Ti^{4+}, Zr^{4+}, Mo^{6+}, or W^{6+}, x = 2–7), hereafter. Undoped $BaTaO_2N$ particles (BTON) and H_2-treated one (BTON:H_2) were also prepared for comparison.[19] In some cases, cobalt oxide cocatalyst (CoO_y, 3 wt. % calculated as Co metal species) was loaded on BTON:M-x particles by impregnation from an aqueous $Co(NO_3)_2$ solution, followed by heating at 673 K for 30 min in air (referred to as CoO_y/BTON:M-x). As-prepared BTON:M-x or CoO_y/BTON:M-x particles were deposited on a Ti substrate (coated area: ca. 1.5×4 cm^2) by electrophoretic deposition method.[18,19,30,31] The representative amount and thickness of the BTON:M-x layer on Ti were ca. 4.0 mg and ca. 2.5 μm, respectively (see Figure S1).[32] Post-necking process was applied to enhance the conductivity among the particles as well as between the particles and the substrate, according to the method shown in our previous reports.[18,19,30,31] As prepared photoanodes will be denoted as BTON:M-x/Ti or CoO_y/BTON:M-x/Ti.

The electrochemical cell used for the photocurrent measurements consisted of a prepared photoanode, a counter electrode (Pt wire), a Ag/AgCl reference electrode, and a Na_2SO_4 solution (0.5M, pH 6). In some cases, a phosphate buffer solution (pH 8), which was prepared by mixing 0.1M Na_2HPO_4aq and 0.1M NaH_2PO_4aq, was employed. The potential of the working electrode was controlled using a potentiostat. The solution was purged with Ar for over 20 min prior to the measurement. The electrodes were irradiated by a 300 W Xe lamp (LX-300F, Cermax) fitted with a cut-off filter (L-42, Hoya) to block the light in the ultraviolet region. The detailed experimental conditions including material synthesis are given in the supplementary material.[32]

Figure 1 shows the XRD patterns of the prepared BTON:Mo-x (x = 2, 5), BTON:Zr-2, BTON:W-2, BTON:Ti-2, and undoped one, in which KCl was used as a standard sample for the correction of 2θ angles. All the samples were identified to the perovskite phase $BaTaO_2N$. The (110) diffraction peak of BTON:Mo shifted to higher angles with increasing amount of Mo^{6+} dopant without emerging any impurity phases, indicating successful replacement of Ta^{5+} (64 pm) by smaller Mo^{6+} (59 pm) up to ca. 5 mol. %. However, further doping of Mo^{6+} resulted in the formation of $BaMoO_4$ phase (see Figure S2).[32] Doping of 2 mol. % of Ti^{4+} or Zr^{4+} resulted in the peak shift to higher or lower angles, respectively, indicating substitution of Ta^{5+} by smaller (Ti^{4+}: 60.5 pm) or larger (Zr^{4+}: 72 pm) cations within the molar ratio up to ca. 2%, while further doping resulted in the formation of Ta_3N_5 impurity phase (see Figures 1 and S2).[32] On the other hand, the main peak of BTON:W-2 was broadened without obvious shifting toward one direction, suggesting that the W cations were introduced not only with the intended valence of W^{6+} (60 pm) but also with other valences such as W^{4+} (66 pm). Particle sizes of the cation-doped samples were not significantly changed from that of the original non-doped one (see Figure S3),[32] while the BTON:Mo-2 sample partially contained larger particles.

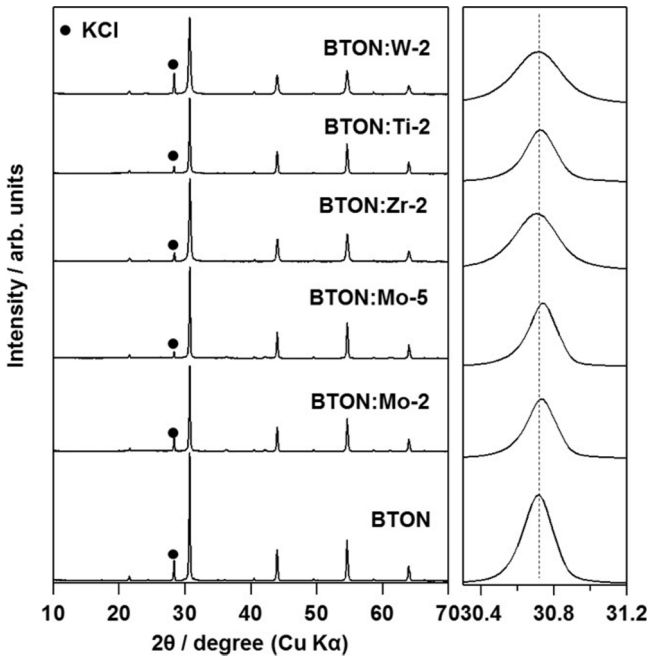

FIG. 1. XRD patterns of BTON, BTON:Mo-x ($x = 2, 5$), BTON:Zr-2, BTON:Ti-2, and BTON:W-2 samples.

Figure 2 shows Mott-Schottky plots of the BTON/Ti, BTON:Mo-x/Ti (x = 2–7), and BTON:Zr-2/Ti electrodes in phosphate buffer solution (pH 8). The donor density (N_D) and the flat band potential (V_f) of these samples were calculated according to the following equation:

$$1/C^2 = 2\,(V - V_f)\,/e\varepsilon_0\varepsilon_r N_D,$$

where C, V, V_f, e, ε_0, ε_r, and N_D denote electrostatic capacity (F m^{-2}), applied potential (V), flat band potential (V), elementary charge (1.602×10^{-19} C), permittivity of vacuum ($8.854 \times$

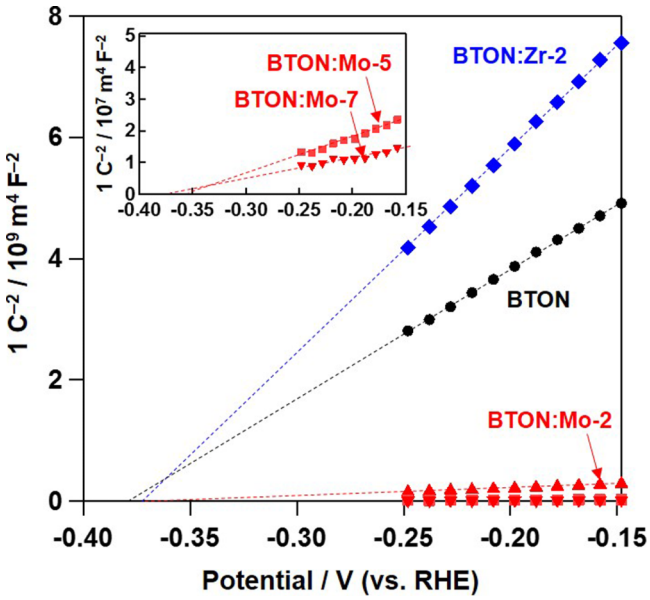

FIG. 2. Mott-Schottky plots of BTON/Ti, BTON:Mo-x/Ti ($x = 2, 5, 7$), and BTON:Zr-2/Ti electrodes. AC amplitude: 10 mV, frequency: 500 Hz.

10^{-12} F m^{-1}), relative permittivity, and donor density (m^{-3}). As for the ε_r of $BaTaO_2N$ semiconductor, one of the reported value (4870) in a previous literature[33] was used in the present study. Based on the equation, the N_D values can be obtained from the slope in Mott-Schottky plots (plot of $1/C^2$ against an appropriate V). Since e, ε_0, and ε_r are constant value, the lower slope value ($2/e\varepsilon_0\varepsilon_r N_D$) means the increase in N_D. The calculated donor density (N_D) and the flat band potential (V_f) for each sample are summarized in Table SI.[32] Although the V_f of these samples (−0.38 to −0.35 V vs. reversible hydrogen electrode (RHE)) were not significantly affected by the cation doping, the N_D were significantly changed, especially by Mo^{6+} doping, as seen in Figure 2 and Table SI.[32] The introduction of Mo^{6+} having higher valence than Ta^{5+} obviously increased the N_D from 1.4×10^{22} m^{-3} (undoped) up to 5.4×10^{24} m^{-3} (at 7 mol. %), while the increase in N_D was not exactly liner to the increased molar amount of Mo^{6+}. The unproportional change in the N_D is probably due to the uncertainness in the C values, which is actually changed by the various factors such as porosity of the samples. On the other hand, the introduction of Zr^{4+} dopant obviously decreased the N_D from 1.4×10^{22} to 8.5×10^{21} m^{-3}. The observed changing trend in the donor density of $BaTaO_2N$ by cation doping (i.e., replacing Ta^{5+} by other tetra or hexahydric-valent cations) is basically similar to that in other metal oxide semiconductors such as $BiVO_4$,[22,24] in which the donor density increased by the substitution of V^{5+} cations by Mo^{6+}.

The influence of the cation-doping on the oxidative photocurrent densities generated by the $BaTaO_2N$/Ti and CoO_y/$BaTaO_2N$/Ti electrodes under visible light irradiation is shown in Figure 3 (see Figures S4 and S5 for the original voltammetric data).[32] The obtained photocurrents were attributed to the competitive reaction of water oxidation and partial self-oxidation of $BaTaO_2N$ surface. The photocurrent density over BTON:Mo photoanodes increased with increasing amount of Mo dopant up to 5 mol. % at whole potential range and then drastically decreased at 7 mol. %. The increased photocurrent densities in the BTON:Mo electrodes are certainly due to the increased donor density, i.e., the decreased electroresistances, in BTON, which will facilitate the electron transfer within the photoanode and consequently increase the photocurrents. The superfluously increased donor density in BTON:Mo-7 will shorten the migration length of holes in the bulk and thus decreased the photocurrent. On the other hand, the performances of BTON:Zr, and BTON:Ti photoanodes were obviously lowered by the introduction of each dopant. The decreased photocurrent with Zr^{4+} doping can be explained by the decreased donor density in BTON. As for the Ti^{4+} doping, reduced Ti^{3+} species might be generated during nitridation, which will simultaneously generate anion defects that increase the donor density but also facilitate the recombination between electrons and holes through the redox cycle. The lowered performance in BTON:W-2/Ti electrode can be explained by the facilitated recombination through the redox cycle between W^{4+} and W^{6+} species.

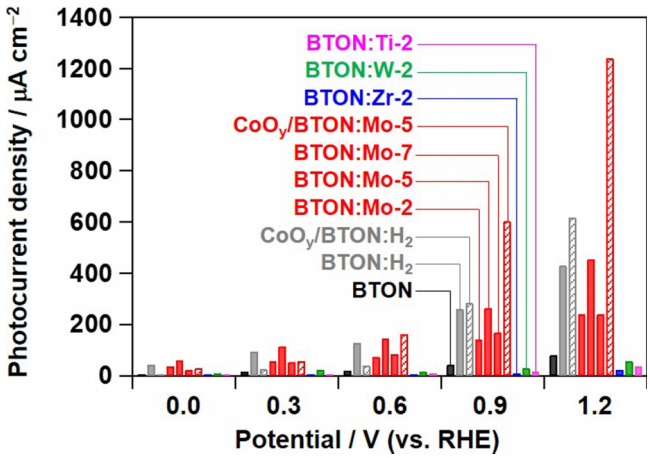

FIG. 3. The influence of the cation-doping on the oxidative photocurrent densities generated by the $BaTaO_2N$/Ti and CoO_y/$BaTaO_2N$/Ti electrodes in an aqueous Na_2SO_4 solution (pH 6) under visible light irradiation ($\lambda > 400$ nm).

As shown above, the doping of 5 mol. % of Mo^{6+} (BTON:Mo-5/Ti) resulted in maximum photocurrent under visible light, which was almost comparable to the previously reported photoanode[19] prepared from H_2-treated $BaTaO_2N$ particles (shown in Figure 3 as BTON:H_2/Ti). Then, the BTON:Mo-5/Ti photoanode was subjected to PEC water splitting coupled with Pt counter electrode for H_2 generation. Similar to the TaON and $BaTaO_2N$ photoanode systems reported previously,[18,19] the loading of the CoO_y cocatalyst was found to be effective to improve the stability of the photoelectrode during the photoirradiation, as well as increasing photocurrent density. As shown in Figures 3 and S5,[32] CoO_y/BTON:Mo-5/Ti showed appreciably higher photocurrent density than the BTON:Mo-5/Ti, indicating that the loaded CoO_y effectively function as cocatalyst that catalyzes water oxidation. The loading of CoO_y on BTON:H_2/Ti was also effective for enhancing the photocurrent, but the degree of enhancement was lower than in the BTON:Mo-5/Ti system, probably due to the decreased amount of anion defects during the impregnation process of CoO_y via calcination in air (at 673 K). As shown in Figure S5,[32] the photocurrent over the unloaded BTON:Mo-5/Ti electrode immediately decreased with photoirradiation, undoubtedly due to the self-oxidative deactivation of the BTON:Mo surface during the photoirradiation, in which holes generated in the BTON:Mo bulk oxidize the nitrogen anion (N^{3-}) to N_2.[34] The loading of CoO_y on BTON:Mo particles prior to the electrode fabrication significantly improved the stability of photocurrent, indicating that the loaded CoO_y efficiently scavenged the holes generated in BTON:Mo bulk and suppressed the self-oxidative deactivation of surface.

Figure 4 shows the incident photon-to-current conversion efficiency (IPCE) action spectra of CoO_y/BTON and CoO_y/BTON:Mo-5 electrodes, along with the photoabsorption spectra (dashed lines) of corresponding powder samples (without CoO_y loading). No significant changes in absorption edge of $BaTaO_2N$ was observed before and after the doping of Mo^{6+} (5 mol. %), indicating the negligible influence of Mo^{5+} doping on the bandgap of $BaTaO_2N$ host. The shapes of the IPCE spectra of both the CoO_y/BTON:Mo-5 and CoO_y/BTON photoanodes were in agreement with those of photoabsorption, indicating that the photocurrents were derived from the band gap transition of $BaTaO_2N$. The CoO_y/BTON:Mo-5/Ti showed much higher IPCE values than the CoO_y/BTON:H_2/Ti, indicating again the positive effect of Mo^{6+} doping.

Figure 5 shows the time courses of H_2 and O_2 evolution over CoO_y/BTON:Mo-5/Ti, CoO_y/BTON:H_2/Ti, and CoO_y/BTON:/Ti photoanodes under visible light irradiation with applied bias of 1.0 V vs. counter electrode. The PEC system of CoO_y/BTON:Mo-5/Ti photoanode generated H_2 and O_2 at close to the stoichiometric ratio (H_2/O_2 = 2); the rate of gas evolutions was much higher than others. The amounts of gases evolved for 180 min (H_2 : 39.0 μmol, O_2: 17.4 μmol) exceeded the molar amounts of BTON:Mo-5 particles (ca. 11.1 μmol) loaded on the Ti substrate, indicating that PEC water splitting proceeded photocatalytically. The faradic efficiencies for H_2 and O_2 evolution were confirmed to be ca. 93% in the reaction, indicating that the most of photogenerated carriers were consumed for PEC water splitting, not for other process such as self-oxidative deactivation.

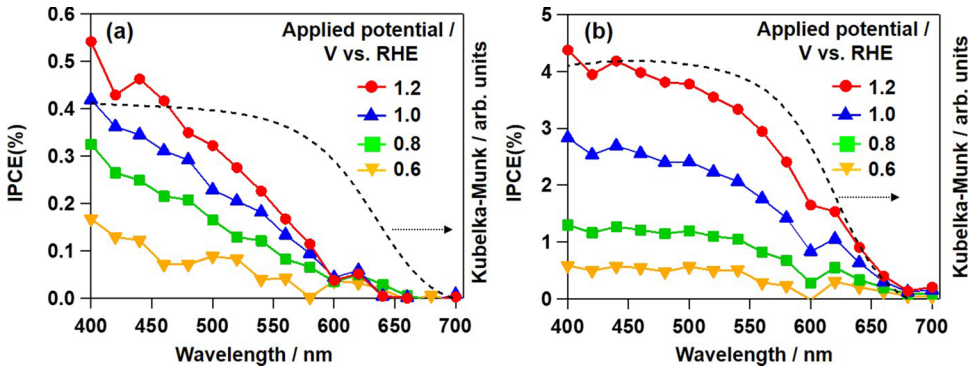

FIG. 4. IPCE spectra of (a) CoO_y/BTON/Ti and (b) CoO_y/BTON:Mo-5/Ti electrodes with various applied potentials (phosphate buffer solution, pH 8), and absorption spectra of (a) BTON and (b) BTON:Mo-5.

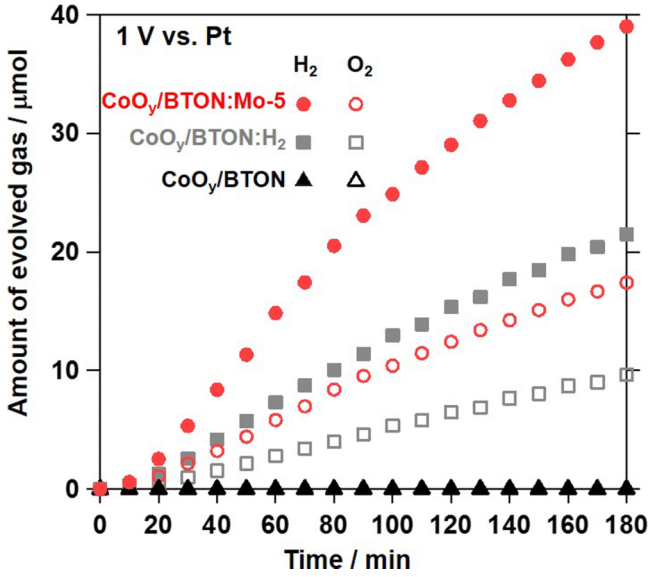

FIG. 5. Time course of gas evolution in two-electrode system composed of CoO_y/BTON:Mo-5/Ti, CoO_y/BTON : H_2/Ti, or CoO_y/BTON/Ti electrode and Pt-wire coated with Cr_2O_3 in phosphate buffer solution (pH 8) under visible light irradiation.

In the present study, the control of donor density of one of the metal (oxy)nitride materials $BaTaO_2N$ was attempted via cation doping for the first time. The partial substitution of Ta^{5+} cations in $BaTaO_2N$ by higher valent Mo^{6+} was found to increase the donor density effectively. The porous photoanode fabricated by Mo-doped $BaTaO_2N$ showed much higher PEC performance under visible light after loading of appropriate cocatalyst, which was also comparable one to the previously reported $BaTaO_2N$ photoanode prepared through pretreatment with H_2 stream at high temperatures. These findings indicated that doping of appropriate metal cation into oxynitride semiconductors was effective for controlling their donor density and achieving efficient PEC water splitting under visible light.

This work was financially supported by the JST-CREST, JSPS-NEXT programs, and JSPS KAKENHI Grant Nos. 15H03849, 15K17896, and 25888013. The authors are also indebted to the technical division of Catalysis Research Center, Hokkaido University for their help in building the experimental equipment.

[1] K. Maeda and K. Domen, J. Phys. Chem. C **111**(22), 7851–7861 (2007).
[2] A. Kudo and Y. Miseki, Chem. Soc. Rev. **38**(1), 253–278 (2009).
[3] M. J. Esswein and D. G. Nocera, Chem. Rev. **107**(10), 4022–4047 (2007).
[4] R. Abe, J. Photochem. Photobiol., C **11**(4), 179–209 (2010).
[5] W. J. Youngblood, S. H. A. Lee, K. Maeda, and T. E. Mallouk, Acc. Chem. Res. **42**(12), 1966–1973 (2009).
[6] G. Hitoki, T. Takata, J. N. Kondo, M. Hara, H. Kobayashi, and K. Domen, Chem. Commun. **2002**(16), 1698–1699.
[7] M. Hara, G. Hitoki, T. Takata, J. N. Kondo, H. Kobayashi, and K. Domen, Catal. Today **78**(1-4), 555–560 (2003).
[8] N. Hara, G. Hitoki, T. Takata, J. N. Kondo, H. Kobayashi, and K. Domen, Stud. Surf. Sci. Catal. **145**, 169–172 (2003).
[9] K. Maeda, M. Higashi, D. L. Lu, R. Abe, and K. Domen, J. Am. Chem. Soc. **132**(16), 5858–5868 (2010).
[10] G. Hitoki, A. Ishikawa, T. Takata, J. N. Kondo, M. Hara, and K. Domen, Chem. Lett. **31**(7), 736–737 (2002).
[11] Y. Lee, K. Nukumizu, T. Watanabe, T. Takata, M. Hara, M. Yoshimura, and K. Domen, Chem. Lett. **35**(4), 352–353 (2006).
[12] G. Hitoki, T. Takata, J. N. Kondo, M. Hara, H. Kobayashi, and K. Domen, Electrochemistry **70**(6), 463–465 (2002).
[13] D. Yamasita, T. Takata, M. Hara, J. N. Kondo, and K. Domen, Solid State Ionics **172**(1-4), 591–595 (2004).
[14] M. Higashi, R. Abe, K. Teramura, T. Takata, B. Ohtani, and K. Domen, Chem. Phys. Lett. **452**(1-3), 120–123 (2008).
[15] S. M. Ji, P. H. Borse, H. G. Kim, D. W. Hwang, J. S. Jang, S. W. Bae, and J. S. Lee, Phys. Chem. Chem. Phys. **7**(6), 1315–1321 (2005).
[16] B. Siritanaratkul, K. Maeda, T. Hisatomi, and K. Domen, ChemSusChem **4**(1), 74–78 (2011).
[17] K. Maeda, M. Higashi, B. Siritanaratkul, R. Abe, and K. Domen, J. Am. Chem. Soc. **133**(32), 12334–12337 (2011).
[18] M. Higashi, K. Domen, and R. Abe, J. Am. Chem. Soc. **134**(16), 6968–6971 (2012).
[19] M. Higashi, K. Domen, and R. Abe, J. Am. Chem. Soc. **135**(28), 10238–10241 (2013).
[20] C. Sanchez, M. Hendewerk, K. D. Sieber, and G. A. Somorjai, J. Solid State Chem. **61**(1), 47–55 (1986).
[21] W. D. Chemelewski, N. T. Hahn, and C. B. Mullins, J. Phys. Chem. C **116**(8), 5256–5262 (2012).
[22] M. L. Zhang, W. J. Luo, Z. S. Li, T. Yu, and Z. G. Zou, Appl. Phys. Lett. **97**(4), 042105 (2010).

[23] A. Kay, I. Cesar, and M. Gratzel, J. Am. Chem. Soc. **128**(49), 15714–15721 (2006).
[24] W. J. Luo, Z. S. Yang, Z. S. Li, J. Y. Zhang, J. G. Liu, Z. Y. Zhao, Z. Q. Wang, S. C. Yan, T. Yu, and Z. G. Zou, Energy Environ. Sci. **4**(10), 4046–4051 (2011).
[25] S. K. Pilli, T. E. Furtak, L. D. Brown, T. G. Deutsch, J. A. Turner, and A. M. Herring, Energy Environ. Sci. **4**(12), 5028–5034 (2011).
[26] L. Chen, F. M. Toma, J. K. Cooper, A. Lyon, Y. J. Lin, I. D. Sharp, and J. W. Ager, ChemSusChem **8**(6), 1066–1071 (2015).
[27] K. Sekizawa, T. Nonaka, T. Arai, and T. Morikawa, Acs Appl. Mater. Interfaces **6**(14), 10969–10973 (2014).
[28] J. Y. Liu, T. Hisatomi, G. J. Ma, A. Iwanaga, T. Minegishi, Y. Moriya, M. Katayama, J. Kubota, and K. Domen, Energy Environ. Sci. **7**(7), 2239–2242 (2014).
[29] M. Higashi, R. Abe, T. Takata, and K. Domen, Chem. Mater. **21**(8), 1543–1549 (2009).
[30] M. Higashi, K. Domen, and R. Abe, Energy Environ. Sci. **4**(10), 4138–4147 (2011).
[31] R. Abe, M. Higashi, and K. Domen, J. Am. Chem. Soc. **132**(34), 11828–11829 (2010).
[32] See supplementary material at http://dx.doi.org/10.1063/1.4931487 for XRD pattern, SEM image, and results of PEC measurement, donor density and flat band potential.
[33] Y. I. Kim, P. M. Woodward, K. Z. Baba-Kishi, and C. W. Tai, Chem. Mater. **16**(7), 1267–1276 (2004).
[34] A. Kasahara, K. Nukumizu, G. Hitoki, T. Takata, J. N. Kondo, M. Hara, H. Kobayashi, and K. Domen, J. Phys. Chem. A **106**(29), 6750–6753 (2002).